Bioresource Technology 111 (2012) 343–352

Contents lists available at SciVerse ScienceDirect

Bioresource Technology

journal homepage: www.elsevier.com/locate/biortech

Harvesting microalgal biomass using submerged microfiltration membranes

M.R. Bilad [a], D. Vandamme [b], I. Foubert [b], K. Muylaert [b], Ivo F.J. Vankelecom [a,*]

[a] Centre for Surface Chemistry and Catalysis, Faculty of Bioscience Engineering, KU Leuven, Kasteelpark Arenberg 23, Box 2461, 3001 Leuven, Belgium
[b] Lab Aquatic Biology, Microbial en Molecular Systems, KU Leuven KULAK, E. Sabbelaan 53, B-8500 Kortrijk, Belgium

ARTICLE INFO

Article history:
Received 14 December 2011
Received in revised form 1 February 2012
Accepted 2 February 2012
Available online 14 February 2012

Keywords:
Microalgae harvesting
Membrane fouling
Chlorella vulgaris
Phaeodactylum tricornutum

ABSTRACT

This study was performed to investigate the applicability of submerged microfiltration as a first step of up-concentration for harvesting both a freshwater green algae species *Chlorella vulgaris* and a marine diatom *Phaeodactylum tricornutum* using three lab-made membranes with different porosity. The filtration performance was assessed by conducting the improved flux step method (IFM) and batch up-concentration filtrations. The fouling autopsy of the membranes was performed by scanning electron microscopy (SEM), energy-dispersive X-ray spectroscopy (EDX) and Fourier transform infrared spectroscopy (FTIR). The cost analysis was estimated based on the data of a related full-scale submerged membrane bioreactor (MBR). Overall results suggest that submerged microfiltration for algal harvesting is economically feasible. The IFM results indicate a low degree of fouling, comparable to the one obtained for a submerged MBR. By combining the submerged microfiltration with centrifugation to reach a final concentration of 22% w/v, the energy consumption to dewater *C. vulgaris* and *P. tricornutum* is 0.84 kW h/m^3 and 0.91 kW h/m^3, respectively.

1. Introduction

Recently, microalgal biomass has been recognized as a promising alternative source of raw material for biofuel production, but a lack of an economical and efficient method to harvest algal biomass is a major drawback to boost their full-scale application (Greenwell et al., 2010). Before entering downstream processing, algal broth normally requires harvesting, up-concentration and drying. At present, microalgae are only produced on a limited scale for high value products, such as food supplements, natural pigments and polyunsaturated fatty acids (Raja et al., 2008). Because of their low concentration in the culture medium (0.5–2 g/l) and small size, typically a few micrometers, harvesting microalgal biomass is a major challenge. Most existing microalgal production systems use energy intensive centrifugation, which represent a major fraction of the total energy demand of the production process (Grima et al., 2003). Hence, the net energy output in the case of biofuel production is seriously decreased.

Membrane technology is generally cheaper than applying centrifuges and is known to be not energy intensive. It thus forms a very promising technology for algal harvesting and additionally offers the advantages of almost complete retention of biomass (Mouchet and Bonnelye, 1998) as well as potential disinfection via removal of protozoa and viruses (Judd, 2006). Furthermore, no chemicals such as coagulants or flocculants are required, thus preventing their accumulation in the biomass or the recycled streams that exist in a coagulation–flocculation process (Vandamme et al., 2011).

Most literature on microalgal harvesting confirms the effectiveness of micro- and ultra-filtration in cross-flow configuration (Rossignol et al., 1991; Zhang et al., 2010). This configuration offers a high productivity due to the high cross-flow velocity and shear rates exposed onto the membrane surface. However, it consumes considerable energy due to high applied pressures and liquid velocities (Le-Clech et al., 2006). Furthermore, over-exposure of microalgal biomass to shear, especially in intake and pumping systems may break microalgal cells to form smaller particles, colloids and dissolved organic matters or promote release of exopolymeric substances (EPS). These small particles are known to cause severe membrane fouling by enhancing pore blocking and producing a less porous cake layer on the membrane surface (Babel and Takizawa, 2010; Ladner et al., 2010). The cell breakage may also lead to the loss of targeted products from the cell interior. Therefore, application of submerged microfiltration that applies lower pressures in absence of any cross flow velocity is expected to be more efficient (Babel and Takizawa, 2010). This system is commonly applied in submerged membrane bioreactors (MBRs) for wastewater treatment, as it is cheaper due to the absence of pressure resistant membrane housings, and proven to offer lower energy consumption (Judd, 2006; Le-Clech et al., 2006). In such immersed system, the shear is generally provided by coarse air bubbles, thus the limited exposure of microalgal cell to enhanced shear rates is also

* Corresponding author. Tel.: +32 16 321594; fax: +32 16 321998.
E-mail address: ivo.vankelecom@biw.kuleuven.be (I.F.J. Vankelecom).

0960-8524/$ - see front matter © 2012 Elsevier Ltd. All rights reserved.
doi:10.1016/j.biortech.2012.02.009

Nomenclature

A	Effective filtration area (m^2)
A_C	Energy consumption for coarse bubble aeration of the referred full-scale MBR installation (0.23 kW h/m^3)
A_n	Membrane area needed (m^2)
A_{ref}	Membrane area of the referenced municipal MBR installation (m^2)
C_a	Energy consumption for compressing the air of the referred full-scale MBR installation (0.02 kW h/m^3)
$CaCO_3$	Calcium carbonate
CIP	Energy consumption for cleaning in place of the referred full-scale MBR installation (0.04 kW h/m^3)
CO_2	Carbon dioxide
CWP	Clean water permeability (l/m^2 h bar)
DMF	N,N-Dimethylformamide
EDX	Energy-dispersive X-ray spectroscopy
EPS	Exopolymeric substances
E_{FS}	Energy consumption for submerged filtration only (kW h/m^3)
E_V	Estimated energy consumption based on permeate volume (kW h/m^3)
E_W	Estimated energy consumption based on dry weight of harvested biomass (kW h/kg)
FTIR	Fourier transform infrared spectroscopy
IFM	Improved flux step method
J	Flux (l/m^2 h)
J_C	Critical flux (l/m^2 h)
J_{Cir}	Critical flux for irreversibility (l/m^2 h)
J_H	High flux (l/m^2 h)
J_L	Low flux (l/m^2 h)
J_{ref}	The referenced flux (22 l/m^2 h)
KBr	Potassium bromid
L	Permeability (l/m^2 h bar)
MBR	Membrane bioreactor
NaClO	Sodium hypochlorite
OD_f	The optical density of the feed
OD_p	The optical density of the permeate
P_{in}	Energy consumption for influent pumping of the referred full-scale MBR installation (0.03 kW h/m^3)
P_P	Energy consumption for permeate pumping of the referred full-scale MBR installation (0.07 kW h/m^3)
PVDF	Polyvinylidene fluoride
PVDF-9	Membrane with 9% PVDF w/w concentration
PVDF-12	Membrane with 12% PVDF w/w concentration
PVDF-15	Membrane with 15% PVDF w/w concentration
PVP	Polyvinylpyrrolidone
r_A	Ratio of membrane area needed (A_n) to the referenced municipal MBR area (A_{ref})
SEM	Scanning electron microscopy
t	Time (h)
TMP	Trans-membrane pressure (bar or kPa).
V	Volume (l)
WC	Wright's cryptophytes medium

Greek symbols

ρ	The solid concentration of microalgae in the feed stream (kg/m^3)
η_a	The harvesting efficiency of microalgal biomass (%)

expected to reduce EPS release and thus to better sustain the filtration operation.

In this study, a submerged microfiltration was applied to harvest both a freshwater microalgal species *Chlorella vulgaris* and a marine diatom *Phaeodactylum tricornutum*. Both *Chlorella* and *Phaeodactylum* are promising species for the production of microalgal biomass for food, feed, or fuel, and are currently intensively studied (Greenwell et al., 2010; Raja et al., 2008). The effect of membrane properties was observed by testing three lab-made polyvinylidene fluoride (PVDF) membranes. The filtration performances were evaluated using the improved flux-step method (IFM) (van der Marel et al., 2009) and batch up-concentration filtrations. The IFM results were used to compare the fouling propensity of the tested membranes for microalgal species, and to provide information on ranges of applicable fluxes in a full-scale system. The membrane fouling was evaluated by observing scanning electron microscopy (SEM) images of fresh, fouled and cleaned membranes and by applying both Fourier transform infrared spectroscopy (FTIR) and energy-dispersive X-ray spectroscopy (EDX) to identify the organic and inorganic fouling, respectively. The energy consumption for a full-scale application of submerged microfiltration process in algae harvesting was also tentatively estimated by adapting the data taken from a related full-scale submerged MBR for wastewater treatment. These values were used as a basis of comparison with other microalgae up-concentration processes.

2. Methods

2.1. Cultivation and characterization of microalgae

C. vulgaris (SAG, Germany, 211-11B) was cultured in Wright's cryptophytes (WC) medium prepared from pure chemicals dissolved in disinfected tap water (Guillard and Lorenzen, 1972). *P. tricornutum* (UGent, Belgium, Pt 86) was cultured in WC medium prepared in deionized water to which 30 g/l synthetic sea salt (Homarsel, Zoutman, Belgium) was added. Both species were grown in two separated plexiglas bubble column photobioreactors, with a working volume of 30 l and diameter of 20 cm. Degassing was carried out with humidified and filtered air at a rate of 5 l/min. The pH was controlled at 8.5 by addition of CO_2 (2–3%) using a pH-stat system. The composition of the freshwater and marine cultivation medium is given in Vandamme et al. (2011). The filtration experiments were performed for 5 days during the stationary growth phase, which was achieved after 7 days of cultivation. Before filtration, the biomass concentration of *C. vulgaris* was 0.41 ± 0.05 g/l and 0.23 ± 0.06 g/l for *P. tricornutum*. Microalgal dry weight was determined gravimetrically by filtration ($n = 3$) using Whatman glass fiber filters (Sigma–Aldrich) and dried until constant weight at 105 °C. For *P. tricornutum*, $(NH_4)_2CO_3$ was used as washing agent (Zhu and Lee, 1997). It is known that the presence of algogenic organic matter, especially exopolysaccharides can cause membrane fouling issues (Ladner et al., 2010). In this experiment, the amount of exopolysaccharides before filtration was determined. For *Chlorella* and for *Phaeodactylum*, respectively 12.7 ± 0.7 mg/l and 13.4 ± 1.0 mg/l EPS was present (measured according to Dubois et al., 1956).

2.2. Membrane preparation and module potting

Three different flat-sheet membranes with different porosity were prepared from 9%, 12% and 15% w/w [PVDF, Mw∼534,000/N,N-Dimethylformamide (DMF)], both Sigma–Aldrich solutions containing polyvinylpyrrolidone (PVP, Mw∼10,000) (Sigma–Aldrich) as an additive via phase inversion. The solution was cast with a 250 μm wet thickness and casting speed of 2.25 cm/s on a polypropylene non-woven support (Novatexx 2471, kindly

supplied by Freudenberg, Germany) and then brought into contact with demineralised water as non-solvent. In the non-solvent bath, the polymer phase separates and solidifies to form a porous membrane. Membrane casting was conducted at 23 °C and 17% relative humidity. The membranes were then stored in tap water before being potted. Two identical sets of membranes were prepared and each set was used for one microalgal species. Fresh membranes were used only for the first filtration and chemically cleaned in between subsequent filtration tests. The polymer concentration in the casting solution of each membrane was further used to index the membranes.

Prior to use, all membranes were potted to form modules with an effective membrane area of 0.016 m^2. A flat-sheet membrane was fixed to a PVC frame by glueing the edges together to form a small envelope using a two-component epoxy glue (UHU-Plus endfest 300, Germany). Both membrane sides were separated by two sheets of spacer in the interior of the module. Permeate was sucked from the module interior through the permeate line. More detailed information about the module potting is available in Bilad et al. (2011).

2.3. Membrane characterization

The microstructure of fresh, fouled and cleaned membranes was analyzed with SEM (Philips SEM XL30 FEG with EDX dx-4i system). The properties of the membranes, i.e., surface pore size, porosity and thickness, were identified with imageJ (NIH, USA) (van der Marel et al., 2010). The clean water permeability (CWP) was measured from coupons with an active filtration surface area of 16.6×10^{-4} m^2 using a standard stainless steel cell with a feed chamber volume of 70 ml. The membrane coupon was supported by a porous stainless steel disk and sealed with O-rings. The filtration was driven by pressurized nitrogen gas. The filtration/applied flux (J) and the permeability (L) of the membrane was calculated by using Eqs. (2) and (3), respectively.

$$J = \frac{V}{At} \quad (\mathrm{l/m^2\ h}) \tag{1}$$

$$L = \frac{J}{\mathrm{TMP}} \quad (\mathrm{l/m^2\ h\ bar}) \tag{2}$$

where V is volume (l), t time (h), A effective filtration area (m^2) and TMP trans-membrane pressure (bar or kPa). Prior to use in the filtration test, all membranes were conditioned by filtering clean water at a flux of 50 L/m^2 h for about 1 h.

To determine the harvesting efficiency of microalgal biomass (η_a), samples were collected at different up-concentration levels. η_a was determined based upon the decrease in optical density of the microalgal suspension between permeate and feed, measured at 550 nm with a Hach Lange DR-2800 spectrophotometer. The η_a (%) was subsequently calculated as suggested by Vandamme et al. (2011):

$$\eta_a = \frac{\mathrm{OD_f} - \mathrm{OD_p}}{\mathrm{OD_f}} \tag{3}$$

where $\mathrm{OD_f}$ is the optical density of the feed and $\mathrm{OD_p}$ the optical density of the permeate.

2.4. Experimental set-up

The filtration performance tests were performed in a lab-scale filtration set-up, illustrated in Fig. 1 (HTML, Belgium) [www.HTML-membrane.be]. The filtration tank has a working volume of 1.5–2.5 l and is equipped with a coarse air bubble aeration located beneath the modules. To allow simultaneous filtration, three modules were fixed into one tank. This allows a correct comparison of membrane performances by applying exactly identical operating and microalgal broth conditions for all tested membranes. Such parallel operation is essential to avoid discrepancies in the feed composition, due to the dynamic behavior of the microalgae over the testing period. Inside the filtration tank, each permeate line was connected through an individual line and an individual vacuum gauge to a separated channel in a multichannel peristaltic pump (Watson-Marlow 205U 16 Channel Pump, UK) using isoprene manifold tubes (Watson-Marlow, UK). The filtration fluxes are adjusted in this case by changing the rotational speed of the pump. For every experiment, three modules with different membranes were installed.

2.5. Membrane filtration

Two different schemes for up-concentration can be implemented by means of membrane filtration. In a continuous process, the microalgae cultivation and the up-concentration process occur in parallel in a separated tank. Therefore, the up-concentration stage can be set independently at a certain value. On the other hand for a batch-wise up-concentration, the broth is up-concentrated up to the desired concentration level after batch cultivation. Both schemes were addressed in this study to assess the filterability of broths. The schematic diagram of the filtration process is shown in Fig 2(A). Three types of filtration tests were conducted during the experiments, namely flux stepping, up-concentration and fixed concentration filtration.

A series of filtration tests was performed using each 25 l initial microalgal broths solution. As shown in Fig. 2(A), two stages of up-concentration were performed in filtration 1 and filtration 2. In filtration 1, 25 l of algae broth (feed 1) was filtered to produce 20 l of permeate 1 and 5 l of retentate 1, which corresponds to a five times up-concentration. In filtration 2, 5 l of retentate 1 was further up-concentrated to produce 3.33 l permeate 2 and 1.67 l of retentate 2. Further up-concentration was not feasible due to the limited amount of microalgal broth.

2.6. Flux-stepping test

In membrane filtration, flux is one of the most important parameters. Higher fluxes normally give higher fouling rates and selecting a filtration flux to allow for a sustained filtration process is always challenging. One of the common ways to define this operational flux is by determining the so called "critical flux" (J_C). The J_C is the maximum flux above which fouling start to become significant for particular feeds and membranes (Le-Clech et al., 2006). The J_C value thus can also be used to compare the fouling propensity of membranes or feeds. The common practice to obtain J_C is to incrementally increase the flux for a fixed duration for each increment, giving a stable TMP at low fluxes but an ever-increasing rate of TMP at fluxes above J_C.

In this study, J_C was obtained by applying the IFM (van der Marel et al., 2009), as illustrated in Fig. 2(B). This method applies successive fluxes (J_H) with increasing level, like in the common flux step method, but includes in addition an intermediate flux decrease to a reference low flux (J_L = 7 l/m^2 h) after each J_H step. J_H was started from 10 l/m^2 h and stepwise increased by 5 l/m^2 h at step durations of 10 min until the maximum speed of the pump (50 l/m^2 h) was reached. At J_L, the convective flow towards the membrane is reduced and due to air scouring, all reversible fouling is removed. This thus gives information about the irreversible fouling rate that later is used to obtain critical flux for irreversibility (J_{Cir}). An arbitrary minimum increase in the TMP of 10 Pa/min was used to determine both J_C and J_{Cir}. The performance of the membranes was evaluated based on both their J_C and J_{Cir} values. Higher Jcs and J_{Cir}s respectively indicate a lower total fouling and

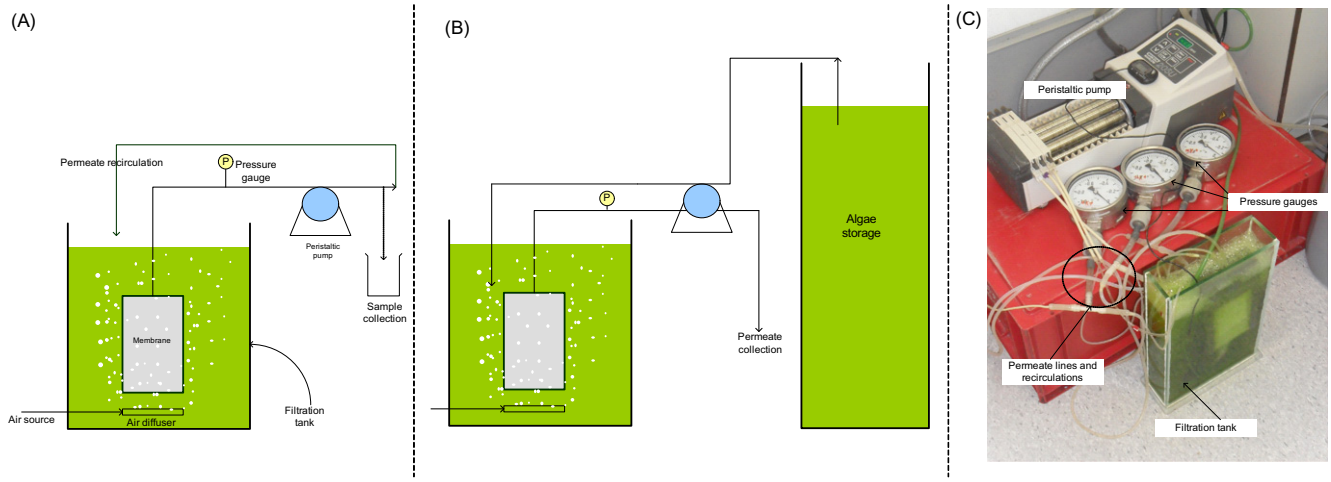

Fig. 1. Experimental set-up for (A) IFM test (B) batch up-concentration and (C) the picture of the set-up.

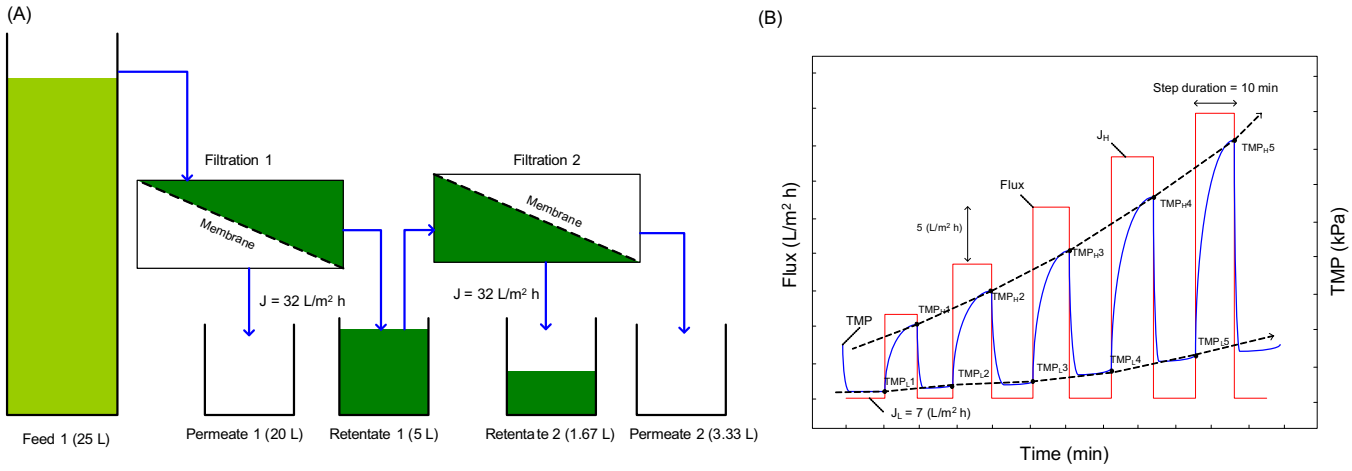

Fig. 2. Membrane filtration: (A) up-concentration (B) illustration of improved flux step method. TMP_H and TMP_L indicate the TMP at the end of J_H and J_L, respectively.

irreversible fouling propensity of the membrane/feed combination. The IFM tests were performed using three different membranes for feed 1, retentate 1 and retentate 2. The results can thus be used to determine the optimum operational flux, membrane and level of first up-concentration using membranes. In practice, a submerged filtration normally operates at sub-critical flux in order to combine the advantages of reasonable productivity with low fouling (Judd, 2006; Le-Clech et al., 2006).

2.7. Up-concentration

The up-concentration filtrations were performed in batch mode, starting from the initial volume to finally reach the requested up-concentration target, as schematically shown in Fig 2(A). The filtration set-up is illustrated in Fig 1(B). The microalgal broth was up-concentrated by filtering it in the filtration tank, which was continuously fed with the fresh broth from the storage tank at the same flow rate as the membrane flux. This way, the volume of broth in the filtration tank was kept constant to ensure constant tank hydrodynamics. The filtration stopped when all microalgal broth from the storage tank was finished. The filtrations were performed at a fixed flux of 32 l/m^2 h and were temporarily stopped for 10 min if the TMP of one or more modules reached±20 kPa to include a membrane relaxation stage. This mode is normally used to limit the fouling for submerged MBRs (Judd, 2006). The system could not be operated at TMP above 25 kPa due to limitations of the set-up. A maximum TMP of 20 kPa is also applied in many fully submerged filtration system using plate-and-frame modules (Judd, 2006).

2.8. Fixed concentration filtration

To study the membrane cleaning and to better characterize the microstructure of the fouled membrane, filtration was performed at a fixed flux of 32 l/m^2 h without relaxation. Retentate 2 was used as feed under conditions of total permeate recycle for 3 h. After the filtration, the membranes were cut into two parts. The first part (without cleaning) was used as the fouled membrane sample, and the second sample (after cleaning) was used as cleaned membrane sample, both for SEM and EDX observations.

2.9. Membrane cleaning and foulant characterization

The membranes were cleaned at the end of each filtration test by flushing them with tap water and soaking them in 1000 ppm sodium hypochlorite (NaClO) solution for 3 h. The microstructure of all fouled membranes was observed from SEM images. Surface analysis of elements was conducted with EDX analysis, integrated in the SEM. This measurement is applied to identify scaling and the formation of salt precipitates on the membrane surfaces. The

membranes were dried and coated with a sputtered gold layer prior to analysis. A part of the cake was analyzed to compare the functional groups present in the cake layer and in the broth. The foulant cake layer was scraped from the fouled membranes after the IFM tests of retentate 2. The broth samples were taken from the feed solution (10 ml). Both were dried at room temperature. Each sample was mixed with potassium bromide (KBr) 10:90 w/w (Fluka), powdered and mechanically pressurized to form the thin films for the FTIR analysis (NICOLET 6700). To identify the specific foulant constituents and their relative quantity, the FTIR spectra were analyzed by their specific absorption peaks.

2.10. Energy consumption

The estimation of the energy consumption for the filtration was based on the energy consumption map of a related full-scale submerged MBR applied in municipal wastewater treatment (Fenu et al., 2010). The overall energy consumption of that full-scale submerged MBR was 0.64 kW h/m^3. This included the energy consumption related to both the bioreactor operation and the submerged microfiltration. By excluding the cost related to the bioreactor operation (such as fine aeration, sludge mixing and disposal, pre-treatment and tank recycle), the energy consumption for a submerged filtration only (E_{FS}), as is the case here for the algae harvesting, would have been 0.40 kW h/m^3. This number still includes influent pumping (P_{in}) (0.03 kW h/m^3 in the full scale municipal MBR), permeate pumping (P_P) (0.07 kW h/m^3), coarse bubble aeration (A_C) (0.23 kW h/m^3), cleaning in place (CIP) (0.04 kW h/m^3) and compressing the air (C_a) (0.02 kW h/m^3). All these operations would also be present in an industrial scale algae harvesting installation.

The energy consumption for microalgae harvesting was estimated by assuming the similar plant scale as for the reference MBR. Since it has a similar capacity, the energy consumption for P_{in} and P_P would also be similar. On the other hand, A_C, C_a and CIP are related to the membrane area and thus a function of the membrane type and its flux for certain feed. Therefore, the ratio (r_A) of membrane area needed (A_n) to the referenced municipal MBR area (A_{ref}), was used to estimate the energy consumption of these three components. Since In the referenced MBR, the operational flux was set at sub-critical value, the applied fluxes (J) (l/m^2 h) for algae harvesting, and the overall energy consumption were calculated using Eqs. (6) and (7).

$$J = 0.85\, J_C \tag{4}$$

$$r_A = \frac{A_n}{A_{ref}} = \frac{J_{ref}}{J} \tag{5}$$

$$E_v = P_{in} + P_P + r_A(A_c + C_a + \mathrm{CIP}) \tag{6}$$

$$E_w = \frac{E_v \eta_a}{\rho} \tag{7}$$

where J_{ref} is the referenced flux of 22 (l/m^2 h), E_v the estimated energy consumption based on the amount of permeating volume (kW h/m^3), E_w the estimated energy consumption based on dry weight of harvested biomass (kW h/kg) and ρ the solid concentration of microalgae in the feed stream (kg/m^3).

3. Results and discussion

3.1. Membrane characterization

The SEM images of the fresh/new membrane surface and the properties of the membranes used in this study are shown in Fig. S1 of supplementary materials and Table 1 respectively. As expected, all membranes have an asymmetric structure as can be seen from the SEM images. The membrane pore size and/or surface porosity, as analyzed by imageJ, decreases with increasing polymer concentration in the casting solutions (van der Marel et al., 2010). A higher polymer concentration leads to an increased polymer volume fraction at the film interface, resulting in a lower porosity and smaller pore sizes. The membranes with larger pore size and/or higher surface porosity show a higher CWP.

The range of the tested membrane pore sizes is far below the size of both microalgal species used in this study and thus easily ensure an almost complete retention of the microalgae. However, smaller sized dissolved nutrients and colloidal particles will pass through the pores. In a continuous operation, this would in addition allow to recycle un-metabolised nutrients, which cannot be achieved in the current flocculation process due to accumulation of flocculants.

It is not clear yet, what the optimum value is for pore size and/or surface porosity. In fact, to realize a complete retention of microalgal cells would be possible with membrane pore sizes just below the size of the microalgal cells, thus ensuring the highest possible fluxes, if combined with high surface porosities and uniform pore size distribution. On the other hand, the membranes with pore size smaller than 0.02 μm can also retain protozoa and viruses, thus preventing contamination on the possibly recycled permeate streams.

3.2. Critical flux and critical flux for irreversibility

Fig. 3 shows the J_C and J_{Cir} for different membranes, different up-concentration levels and different microalgal species. The upward arrow (↑) indicates that the maximum flux of 50 l/m^2 h of the pump was exceeded. The critical fluxes were determined after each stage of the subsequent up-concentration filtrations. The membranes were cleaned in between each experiment. Since the results show that J_C or J_{Cir} values often exceed the maximum applicable flux, the build-up TMP during the filtrations at Fig. 4 can also be directly used for comparison. It was not possible to apply multiple IFM tests or replicates due to the limited amount of sample. Therefore, a statistical analysis could not be provided in this study and interpretation of the data will only be done in general terms, based on data trends that are clear enough. An extensive study with statistical analysis using a high-throughput reactor approach, as suggested by Bilad et al. (2011), is necessary to better understand these cases.

3.2.1. Role of pore size and surface porosity

The critical J_C and J_{Cir} increase with the increase of membrane pore size and/or surface porosity, i.e. from membrane PVDF-15 over PVDF-12 to PVDF-9. This trend is very clear, especially for the *C. vulgaris* broth. A lower local flux (i.e. amount of liquid passing through a single pore) and a lower feed retention are expected for the larger pores. For most conditions applied, the J_{Cir} were exceeding the maximum J_H, representing the very low fouling tendency of the membranes under the given submerged conditions.

3.2.2. Influence of feed

A clear influence from the up-concentration level on the J_C and J_{Cir} is shown in Fig. 3. The more concentrated the microalgae solution, the higher the tendency to foul the membrane surface, as reflected in the lower J_cs and J_{Cir}s for as far as detectable. This is very obvious for *C. vulgaris* broths which have higher solid concentrations, which occurred for both J_C and J_{Cir}. For the *P. tricornutum* species, J_Cs are the same for retentates 1 and 2 for all quasi membranes. They are in general lower than the J_C of feed 1. From the TMP profiles obtained with *P. tricornutum*, it is obvious that

Table 1
Summary of membranes properties.

Membranes	Pore size (μm)	Surface porosity (%)	Clean water permeability (l/m^2 h bar)
PVDF-9	0.036	29	6291 ± 900
PVDF-12	0.013	19.2	5345 ± 426
PVDF-15	0.008	18.3	3457 ± 981

for all membranes the TMP of retentate 2 is always lower than for retentate 1 as shown in Fig. 4. This can be explained by the relatively low solid concentration of the broth.

No clear trends for J_{Cir} for PVDF-9 and PVDF-12 can be given since no TMP build-up was observed during the IFM test. Apparently, the irreversible fouling rate was too low to be detected by the vacuum gauge. This very high J_{Cir} implies that membrane filtration for microalgal harvesting at very high operational fluxes might be feasible with an expected low degree of irreversible fouling. This should keep investment costs low (lower membrane area to be installed) and even further decrease energy cost (less aeration per volume treated and less frequent cleaning).

3.2.3. Microalgal species

The values of J_C and J_{Cir} for *P. tricornutum* are slightly higher than for *C. vulgaris* at all up-concentration levels. Initially, it was expected that *P. tricornutum* would have a more important fouling tendency, judging from the fusiform shape compared to the round shape of *C. vulgaris*. However, this was not observed during this study, possibly due to lower solid concentration of the *P. tricornutum* broth (*x* compared to *y* for *C. vulgaris*) that diminishes this effect. The effect of EPS concentration could not be evaluated in this study, since the initial EPS concentration for both microalgal broths was at a similar magnitude of 12.7 and 13.3 mg/l for *C. vulgaris* and *P. tricornutum*, respectively.

The results from the IFM revealed the clear dependency of the J_C and J_{Cir} on up-concentration level and the membrane pore size and/or surface porosity. Within the applied up-concentration levels, the J_Cs are relatively higher than the ones obtained for activated sludge filtration (Satyawali and Balakrishnan, 2008). Consequently, higher operational fluxes for microalgal harvesting are expected, even though the range of the up-concentrations in this study was rather limited. The filtration at higher up-concentration levels is preferable to achieve a higher degree of dewatering. There must be a trade-off between up-concentration level and fouling to obtain the most economical objective. Most probably, a hybrid process with an initial dewatering via membrane filtration followed by a further dewatering via centrifuges could be optimal.

3.3. Up-concentration

Apparently, applying the relaxation mode is beneficial for an optimum algae harvesting process, as shown in Fig. 5. Intermittent stopping of the filtration in a so-called relaxation operation mode was found sufficient to restore the performance. The preliminary results suggest that a membrane with a bigger pore size is most efficient for the batch up-concentration processes studied here. The profiles for *P. tricornutum* are in agreement with the J_C. The membranes with a lower J_C experience a higher fouling when all membranes are operated at a similar flux. Above the J_C, the formation of cake or gel on the membrane surface is expected (van der Marel et al., 2009). Since the applied filtration flux was above the J_C for PVDF-15, rapid fouling was indeed observed. For PVDF-9 and 12, the flux was below their J_C, leading to a more sustained filtration. A surprising result is observed for the up-concentration of

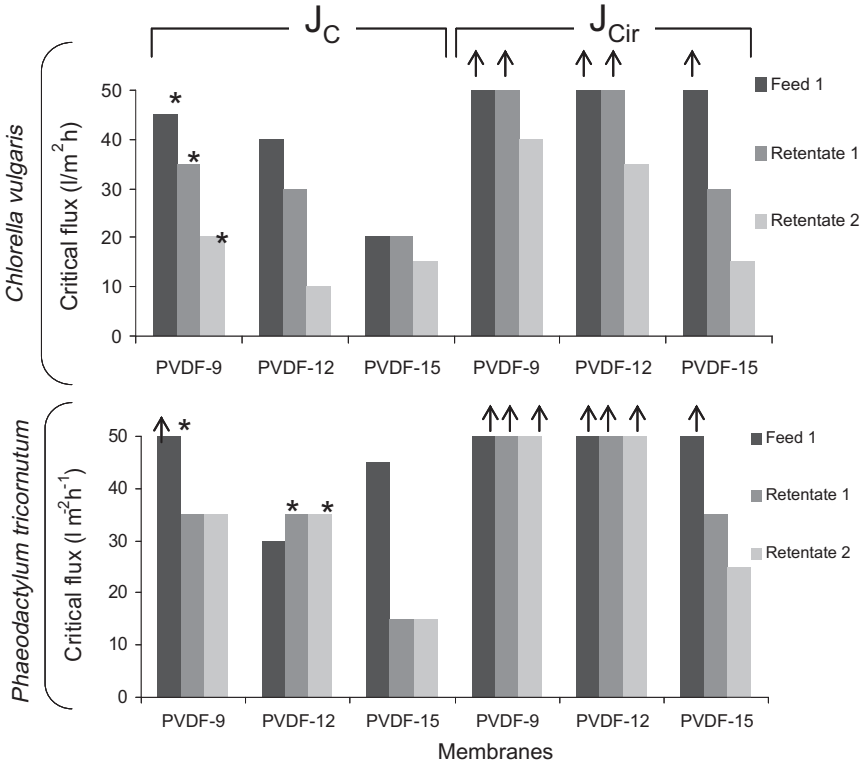

Fig. 3. Critical flux (J_C) and critical flux for irreversibility (J_{Cir}) of different membranes for different feed solutions. (*membranes used for energy consumption estimation). The arrows (↑) indicate that the value is more than 50 l/m^2 h.

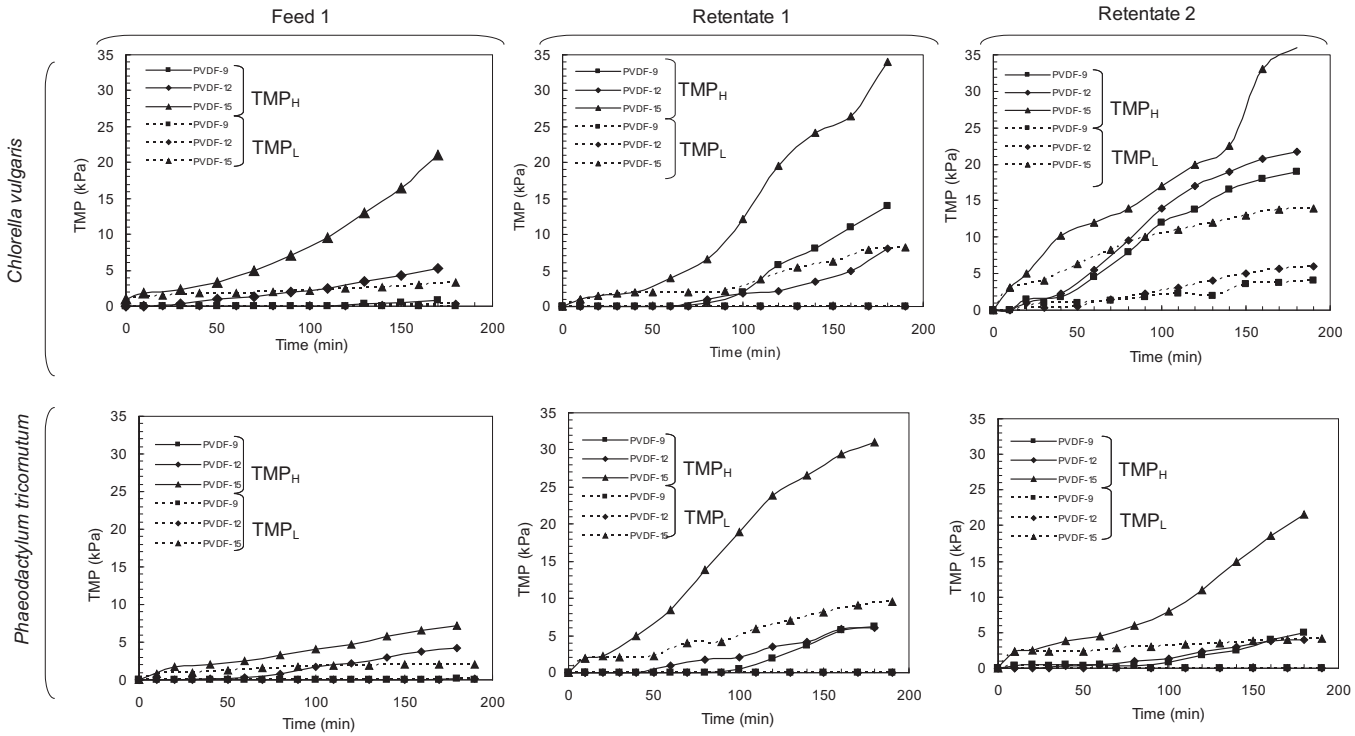

Fig. 4. The flux stepping profile of both microalgal broth filtrations at different up-concentration level. TMP_H and TMP_L indicate the TMP at the end of J_H and J_L, respectively.

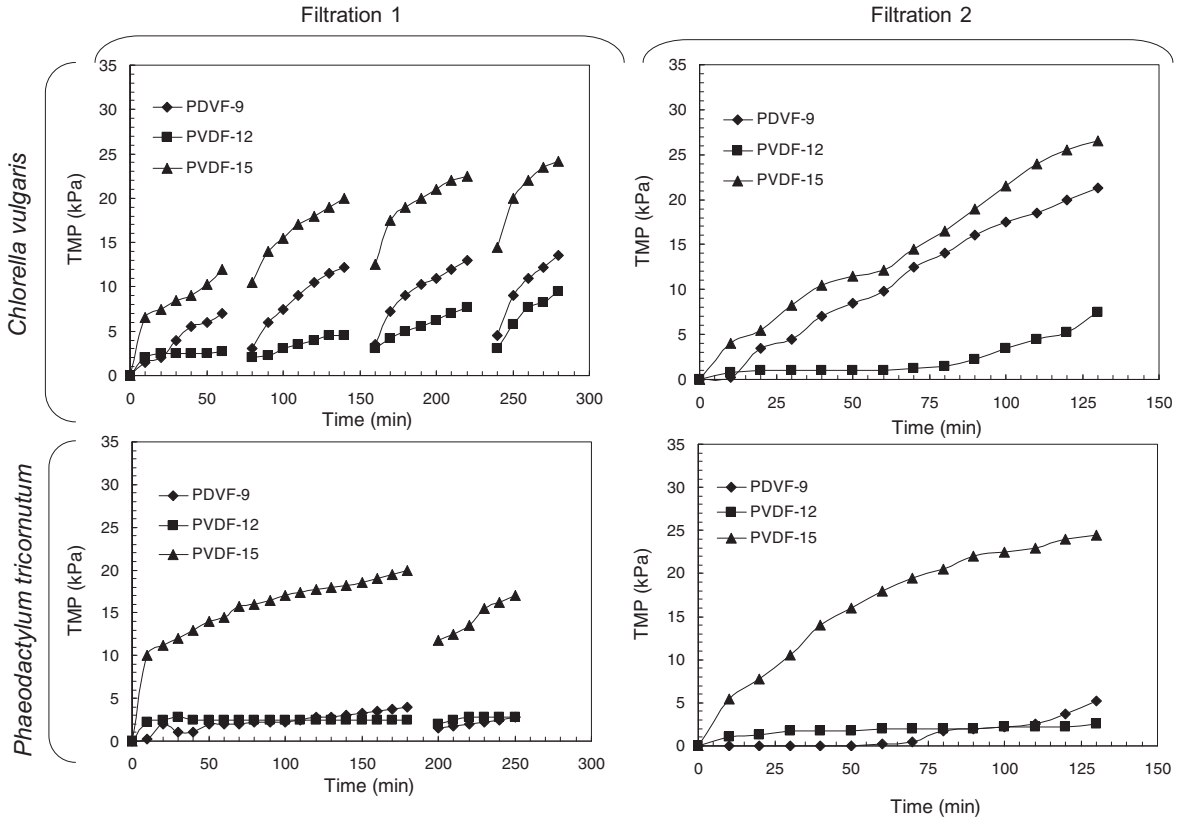

Fig. 5. The TMP build-up during the up-concentration of both microalgal broths. (Notice the larger *x*-axis scale for filtration 1).

the *C. vulgaris* broth. PVDF-12 that has a lower J_C experienced a lower fouling tendency compared to PVDF-9, for which no explanation can be given at this time.

The result from the up-concentration filtration suggests that, membranes with larger pore size and higher surface porosity show lower tendency of fouling. This is also in line with the results of

IFM test. However, the maximum degree of up-concentration could not be attained in this study due to the limited availability of samples. The fouling that occurred during a long run up-concentration process could be partly controlled by applying intermittent filtration and by applying maintenance and intensive cleanings as commonly practiced in MBRs for wastewater treatment (Judd, 2006).

3.4. Fouling autopsy and membrane cleaning

The SEM images of the fouled membranes are shown in Fig. S1. The fouled membrane samples were taken after 3 h of continuous filtration with the most concentrated feed (retentate 2) under conditions of total permeate recycle. Observations on SEM images at lower magnification revealed a non-homogeneous distribution of deposited cells. The visible defects on the membrane surface are most probably caused during the SEM sample preparations, involving drying, and not by the filtration operation (Cui et al., 2003; Genkin et al., 2006).

Fig. S1 shows the deposited *C. vulgaris* cells on the membrane surface. The microalgal cells form small clusters that eventually may initiate biofilm formation. The sticky gel-like EPS on the cell walls may be the cause of membrane pore blocking around the cell and/or cell clusters, resulting in a significant barrier to permeate flow. In addition, they also might provide a highly hydrated gel matrix in which other microorganisms are embedded (Chang et al., 2002). No signs of algae compaction can be observed for *C. vulgaris*, most probably due to the relatively low applied TMP (<25 mbar). This is in contrast with observation under cross flow configuration, where much higher TMPs (2–3 bar) are generally applied (Babel and Takizawa, 2010).

A relatively small amount of *P. tricornutum* is deposited on the membrane surface, especially for PVDF-9 and 12. This may be due to the lower solid concentration of this algae broth in reported experiments. Over the filtration period, the TMP increased up to 25 kPa where compaction of the deposited cells eventually occurred. The gel-like substances are also clearly seen in the filtration using PVDF-15 where the released EPS from the deposited cells could block the pores.

The FTIR spectra of the bulk broths and the cake layers scraped from the surface of the fouled membranes given in Fig. S2 of supplementary materials, show a variety of foulant components that are mostly found in natural organic matter. The broad peak present at 1000–1200 cm^{-1} is due to the symmetric and asymmetric C=O stretches in polysaccharides or polysaccharide-like substances. The peak around 1400 cm^{-1} is attributed to symmetrical stretches of –COO– associated with amino acids (Omoike and Chorover, 2004). Two peaks at 1652 and 1540 cm^{-1} are unique to protein secondary structures, called amides I and II, or are assigned in some cases to humic-like substances (Kimura et al., 2005). A sharp peak at 1740 cm^{-1} is associated with the C=O ester group and two peaks at 2854 and 2925 cm^{-1} are associated with CH_2 and CH_3 stretchings, all primarily from lipids and fatty acids (Dean et al., 2010). Meanwhile, very broad peaks between 3000 and 3600 cm^{-1} originate from O–H stretching, mainly from water.

The SEM images of the fouled and the cleaned membranes in Fig. S1 also show deposited crystals on the membrane surface, representing the inorganic fouling or scaling. It is even more obvious in the images obtained at lower magnifications. The size of the crystals is heterogeneous, and goes up to 5 μm. These crystals block the surface pores and reduce the permeability. The formation of the crystals was not observed on the internal structure of the membranes, observed from SEM images of membrane cross-section (data not shown), thus indicating their retention by the membrane. More detailed observations show that the crystals form different shapes, typical for mineral scale deposit (Tzotzi et al., 2007).

EDX analysis spotted on the crystal shows that they mainly consist of calcium (data not shown). The crystals thus most probably comprised $CaCO_3$. The high amount of crystals is quite surprising due to the relatively low calcium concentrations in both broth solutions, 2.7 and 9.1 mM for *C. vulgaris* and *P. tricornutum* respectively. The nucleation of $CaCO_3$ crystals may be started at the beginning of the filtration and further develop over the filtration period (5 days). In the long-term, the growth of crystals could accelerate and intensify the inorganic fouling. The size of the $CaCO_3$ crystals tends to be deformed compared with the initial rhombohedral shape, as also found by Tzotzi et al. (2007). Obviously, the air scouring was unable to remove this type of scaling. The calcium ions can interact with EPS as Ca bridges to further accelerate the biofilm formation on the membrane surface (Yan et al., 2010).

The SEM images of the membranes after cleaning with NaOCl are shown in Fig. S1. Most of the organic foulants were removed, but only limited removal of the crystals was observed, as expected. Indeed, as an oxidant, NaOCl removes organics (Tzotzi et al., 2007), but shows little impact on inorganic scaling. Similar phenomena were also found by Lee and Kim (2009) and Yan et al. (2010) for cleaning a fouled MBR membrane treating calcium-rich wastewaters. They suggested to apply citric acid to effectively remove the inorganic scaling from the membrane surfaces, which can also be suggested for further study of the microalgal harvesting process.

The SEM images of fouled and cleaned membranes show that inorganic was more dominant than organic fouling. However, a low impact of inorganic fouling on permeability was observed, because the crystals are not compressible and only partially block the pores. The formation of inorganic scaling was unexpected due to only 3 h of filtration time before the membranes were cut for the SEM observation. It is not clear whether the crystals were only formed during the drying process for the SEM sample preparation, or during the actual filtration, due to the relatively low calcium concentration in the broth. During the drying process for the FTIR samples, the presence of crystals in the dried broth was visible for both microalgal broths. However, if the crystals were formed during the drying of samples, a lot of NaCl crystals would also be expected due to its high concentration (1.8 mM for the *C. vulgaris* broth and 442.1 mM for the *P. tricornutum* broth). It is also possible that the inorganic precipitation accumulated during the whole filtration experiments, since the cleaning was not effective enough to remove them from the membrane surfaces. To prove this, the application of environmental scanning electron microscopy, where dried sample are not required, is suggested in further studies (Meng et al., 2010).

An inherent drawback of the submerged aerated systems is the non-homogeneous distribution of the air bubbles (Meng et al., 2010; Satyawali and Balakrishnan, 2008), especially at lab scale. It leads to a heterogeneous shear rate across the membrane surface. The parts of surfaces that experience less or even no aeration are fouled faster, leaving the remaining surface to filter at higher local fluxes, thus inducing a TMP jump later. Therefore, the application of the more advanced fouling limitation techniques, such as vibration module is expected to give better performances (Bilad et al., 2012). In addition, aeration can also be provided from CO_2 enriched air stream. In this way, coarse bubbles not only induces shear rate, but also supplies adequate inorganic carbon to the microalgae and lowers the pH of the broth, thus minimizing the scaling. Therefore, the cost associated with the coarse bubble aeration can be combined with the cost to provide CO_2 as carbon source for the growth of microalgae.

3.5. Harvesting efficiency and energy consumption

The harvesting efficiency of membrane filtrations using different membranes and up-concentration levels for both microalgae

Table 2
Harvesting efficiency and energy consumption for algae harvesting using submerged filtrations, expressed per volume of permeate and per weight of algae harvested.

Algae species	Feed	ρ (kg/m^3)	Harvesting efficiency			Energy consumption			
			PVDF-9	PVDF-12	PVDF-15	Membrane	J (l/m^2 h)	E_V (kW h/m^3)	E_W (kW h/kg)
Chlorella vulgaris	Feed 1	0.4	98%	98%	98%	PVDF-9	38.3	0.27	0.64
	Retentate 1	1.8	92%	82%	98%	PVDF-9	29.8	0.31	0.59
	Retentate 2	3.5	99%	99%	100%	PVDF-9	17.0	0.48	1.10
Phaeodactylum tricornutum	Feed 1	0.2	70%	77%	90%	PVDF-9	42.5	0.25	0.98
	Retentate 1	0.7	93%	99%	99%	PVDF-12	29.8	0.31	1.32
	Retentate 2	2.0	99%	99%	98%	PVDF-12	29.8	0.31	1.29

are shown in Table 2. Almost complete algae retention was achieved for all membranes and up-concentration levels. This magnitude is commonly achieved using ultra- or microfiltration membranes (Mouchet and Bonnelye, 1998; Rossignol et al., 1991). The observed few efficiencies below 90% are most probably due to occasional defects in the membranes or their potting. The comparison of concentration factor based ρ for 5 and 15 times up-concentrated broths found that that their values were 4.4 and 8.5 times and 4.4 and 12.7 times for *C. vulgaris* and *P. tricornutum* respectively. These lower values compared to volumetric up-concentration are due to non-retained biomass that pass through the membrane and due to washout of biomass during the membrane cleaning.

Table 2 also shows the estimation of the energy consumption for reported use of submerged membranes. Results show that the filtration performance, represented by the applied fluxes, is a very crucial parameter. It would thus be of key importance to have high-flux membranes, possibly adapted for this type of filtration. In addition, the up-concentration level also clearly affects the energy consumption, especially based on dry weight of harvested biomass. It will be very crucial decision to what level up-concentration will take place and whether a hybrid process, e.g. with centrifugation as final up-concentration technology, will be more preferred. At lower concentrations, the harvested biomass is less for a given specific filtration volume. Comparing the two microalgal species, the energy consumption is of a similar magnitude, in line with the results of the filterability tests.

In general, the submerged microfiltration offers a relatively low energy consumption, based on the present study. The lowest energy consumptions obtained were 0.27 and 0.25 kW h/m^3, and corresponding to 0.64 and 0.98 kW h/kg for *C. vulgaris* and *P. tricornutum* respectively. For similar microalgal species, electro coagulation flocculation requires 1.3–9.5 and 0.2–0.4 kW h/kg, depending on the applied current density (Vandamme et al., 2011). This value is even more promising when compared with a centrifugation process, which typically consume about 8 kW h/m^3, which makes centrifugation only economically feasible for high value applications (Danquah et al., 2009). However, it has to be noticed that the energy consumption numbers presented are only rough estimation from the data obtained at a relatively very short experimental time with a full-scale MBR on domestic wastewater as a reference. The test for a continuous harvesting process by combining a photo-bioreactor with a submerged filtration is still required to confirm the results. Estimation on operational expenses for membrane filtration is very scale-dependent. For instance, the real energy consumption of membrane aeration for a pilot scale submerged MBR was 5–6 kW h/m^3 (Gil et al., 2010) but significantly lower (0.23 kW h/m^3) for a full-scale plant (Fenu et al., 2010).

The final concentrations obtained after 15 times up-concentration are rather low. However, if the submerged filtration is combined with centrifugation, a final concentration of 22% w/v could be achieved. By assuming a complete microalgae rejection and by adopting the data from Table 2 for retentate 2, the energy consumption for dewatering of *C. vulgaris* and *P. tricornutum* would be 0.84 kW h/m^3 and 0.91 kW h/m^3, respectively. The calculation was obtained by assuming that the initial concentrations to be equal to that of feed 1 and the final concentration to be 22% w/v. These values are far below the energy consumption using polymeric flocculation (14.81 kW h/m^3), vacuum filters (5.9 kW h/m^3), tangential flow filtration (2.06 kW h/m^3) and a single step centrifugation (8 kW h/m^3), as estimated by Danquah et al. (2009). These low values are achieved since most of microalgal broth volume are filtered within the first 15 times up-concentration (93.3%) leaving the rest (6.7%) for the higher cost centrifugation.

4. Conclusions

This study reveals the potential of submerged microfiltration as a low-cost microalgae harvesting process. The IFM results suggest lower degrees of fouling compared to conventional submerged MBRs within the range of operational parameters. The energy estimation gave a promising prospect for this technology to be applied at larger scales as a low-cost and energy efficient technology. Furthermore, it widens the possibility to apply microalgae technology both for high and low value products. Further filtration studies on longer-term continued microalgal harvesting at still higher up-concentration levels, and combined in hybrid processes are still necessary.

Acknowledgements

K.U.Leuven for support in the frame of the CECAT excellence, GOA, FWO (G.0808.10 N) and IDO financing, and the Flemish Government for the Methusalem funding and the Federal Government for an IAP grant.

Institute for the promotion of Innovation by Science and Technology-Strategic Basic Research (IWT-SBO) project Sunlight and the K.U.Leuven Research Coordination Office-Industrial Research Fund (DOC-IOF) project Algae-Tech

Appendix A. Supplementary data

Supplementary data associated with this article can be found, in the online version, at doi:10.1016/j.biortech.2012.02.009.

References

Babel, S., Takizawa, S., 2010. Microfiltration membrane fouling and cake behaviour during algal filtration. Desalination 261, 46–51.

Bilad, M.R., Declerck, P., Piasecka, A., Vanysacker, L., Yan, X., Vankelecom, I.F.J., 2011. Development and validation of a high-throughput membrane bioreactor (HT-MBR). J. Membr. Sci. 379, 146–153.

Bilad, M.R., Mezohegyia, G., Declerck, P., Vankelecom, I.F.J., 2012. Novel magnetic vibrating membrane for fouling control in membrane bioreactors. Wat. Res. 46, 63–72.

Chang, I.S., Le-Clech, P., Jefferson, B., Judd, S., 2002. Membrane fouling in membrane bioreactors for wastewater treatment. J. Environ. Eng. 128, 1018–1029.

Cui, Z.F., Chang, S., Fane, A.G., 2003. The use of gas bubbling to enhance membrane processes. J. Membr. Sci. 221, 1–35.

Danquah, M.K., Ang, L., Uduman, N., Moheimani, N., Forde, G.M., 2009. Dewatering of microalgal culture for biodiesel production: exploring polymer flocculation and tangential flow filtration. J. Chem. Technol. Biotechnol. 84, 1078–1083.

Dean, A.P., Sigee, D.C., Estrada, B., Pittman, J.K., 2010. Using FTIR spectroscopy for rapid determination of lipid accumulation in response to nitrogen limitation in freshwater microalgae. Bioresour. Technol. 101, 4499–4507.

Dubois, M., Gilles, K.A., Hamilton, J.K., Rebers, P.A., Smith, F., 1956. Colorimetric method for determination of sugars and related substances. Anal. Chem. 28, 350–356.

Fenu, A., Roels, J., Wambecq, T., De Gussem, K., Thoeye, C., De Gueldre, G., Van De Steen, B., 2010. Energy audit of a full scale MBR system. Desalination 262, 121–128.

Genkin, G., Waite, T.D., Fane, A.G., Chang, S., 2006. The effect of vibration and coagulant addition on the filtration performance of submerged hollow fibre membranes. J. Membr. Sci. 281, 726–734.

Gil, J.A., Túa, L., Rueda, A., Montaño, B., Rodríguez, M., Prats, D., 2010. Monitoring and analysis of the energy cost of an MBR. Desalination 250, 997–1001.

Greenwell, H.C., Laurens, L.M.L., Shields, R.J., Lovitt, R.W., Flynn, K.J., 2010. Placing microalgae on the biofuels priority list: a review of the technological challenges. J. R. Soc. Interface 7, 703–726.

Grima, E.M., Belarbi, E.H., Fernandez, F.G.A., Medina, A.R., Chisti, Y., 2003. Recovery of microalgal biomass and metabolites: Process options and economics. Biotechnol. Adv. 20, 491–515.

Guillard, R., Lorenzen, C., 1972. Yellow-green algae with chlorophyllide. J. Phycol. 8, 10–14.

Judd, S., 2006. The MBR Book: Principles and Applications of Membrane Bioreactors in Water and Wastewater Treatment, first ed. Elsevier, Amsterdam Boston London.

Kimura, K., Yamato, N., Yamamura, H., Watanabe, Y., 2005. Membrane fouling in pilot-scale membrane bioreactors (MBRs) treating municipal wastewater. Environ. Sci. Technol. 39, 6293–6299.

Ladner, D.A., Vardonaand, D.R., Clark, M.M., 2010. Effects of shear on microfiltration and ultrafiltration fouling by marine bloom-forming algae. J. membr. Sci. 356, 33–43.

Lee, M., Kim, J., 2009. Membrane autopsy to investigate $CaCO_3$ scale formation in pilot-scale, submerged membrane bioreactor treating calcium-rich wastewater. J. Chem. Technol. Biotechnol. 84, 1397–1404.

Le-Clech, P., Chen, V., Fane, T.A.G., 2006. Fouling in membrane bioreactors used in wastewater treatment. J. Membr. Sci. 284, 17–53.

Meng, F., Liao, B., Liang, S., Yang, F., Zhang, H., Song, L., 2010. Morphological visualization, componential characterization and microbiological identification of membrane fouling in membrane bioreactors (MBRs). J. Membr. Sci. 361, 1–14.

Mouchet, P., Bonnelye, V., 1998. Solving algae problems: French expertise and worldwide applications. J. Water SRT-Aqua. 47, 125–141.

Omoike, A., Chorover, J., 2004. Spectroscopic study of extracellular polymeric substances from *Bacillus subtilis*: aqueous chemistry and adsorption effects. Biomacromolecules. 5, 1219–1230.

Raja, R., Hemaiswarya, S., Kumar, N.A., Sridhar, S., Rengasamy, R., 2008. A perspective on the biotechnological potential of microalgae. Crit. Rev. Microbiol. 34, 77–88.

Rossignol, N., Vandajon, L., Jaouen, P., Quemeneur, F., 1991. Membrane technology for the continuous separation microalgae/culture medium: compared performances of cross-flow microfiltration and ultrafiltration. Aquacult. Eng. 20, 191.

Satyawali, Y., Balakrishnan, M., 2008. Treatment of distillery effluent in a membrane bioreactor (MBR) equipped with mesh filter. Sep. Purif. Technol. 63, 278–286.

Tzotzi, C., Pahiadaki, T., Yiantsios, S.G., Karabelas, A.J., Andritsos, N., 2007. A study of $CaCO_3$ scale formation and inhibition in RO and NF membrane processes. J. Membr. Sci. 296, 171–184.

Vandamme, D., Pontes, S.C., Goiris, K., Foubert, I., Pinoy, L.J., Muylaert, K., 2011. Evaluation of electro-coagulation-flocculation for harvesting marine and freshwater microalgae. Biotechnol. Bioeng. 108, 2320–2329.

van der Marel, P., Zwijnenburg, A., Kemperman, A.J.B., Wessling, M., Temmink, H., van der Meer, W.G.J., 2009. An improved flux-step method to determine the critical flux and the critical flux for irreversibility in a membrane bioreactor. J. Membr. Sci. 332, 24–29.

van der Marel, P., Zwijnenburg, A., Kemperman, A.J.B., Wessling, M., Temmink, H., van der Meer, W.G.J., 2010. Influence of membrane properties on fouling in submerged membrane bioreactors. J. Membr. Sci. 348, 66–74.

Yan, X., Gerards, R., Vriens, L., Vankelecom, I., 2010. Hollow fiber membrane fouling and cleaning in a membrane bioreactor for molasses wastewater treatment. Desalin. Water Treat. 18, 192–197.

Zhang, X., Hu, Q., Sommerfeld, M., Puruhito, E., Chen, Y., 2010. Harvesting algal biomass for biofuels using ultrafiltration membranes. Bioresour. Technol. 101, 5297–5304.

Zhu, C.J., Lee, Y.K., 1997. Determination of biomass dry weight of marine microalgae. J. Appl. Phycol. 9, 189–194.